General and Comparative Endocrinology 229 (2016) 8–18

Contents lists available at ScienceDirect

General and Comparative Endocrinology

journal homepage: www.elsevier.com/locate/ygcen

Production of recombinant insulin-like androgenic gland hormones from three decapod species: *In vitro* testicular phosphorylation and activation of a newly identified tyrosine kinase receptor from the Eastern spiny lobster, *Sagmariasus verreauxi*

Joseph Aizen [a,1], Jennifer C. Chandler [a,1], Quinn P. Fitzgibbon [b], Amir Sagi [c], Stephen C. Battaglene [b], Abigail Elizur [a], Tomer Ventura [a,*]

[a] Faculty of Science, Health, Education and Engineering, GeneCology Research Centre, University of the Sunshine Coast, Queensland 4558, Australia
[b] Fisheries and Aquaculture, Institute for Marine and Antarctic Studies, University of Tasmania, Hobart, Tasmania, Australia
[c] Department of Life Sciences and The National Institute for Biotechnology in the Negev, Ben-Gurion University of the Negev, Beer-Sheva, Israel

ARTICLE INFO

Article history:
Received 5 November 2015
Revised 5 February 2016
Accepted 12 February 2016
Available online 13 February 2016

Keywords:
Insulin-like androgenic gland hormone
Tyrosine kinase receptor
Phosphorylation
Spiny lobster
Decapod

ABSTRACT

In crustaceans the insulin-like androgenic gland hormone (IAG) is responsible for male sexual differentiation. To date, the biochemical pathways through which IAG exerts its effects are poorly understood and could be elucidated through the production of a functional recombinant IAG (rIAG). We have successfully expressed glycosylated, biologically active IAG using the *Pichia pastoris* yeast expression system. We co-expressed recombinant single-chain precursor molecules consisting of the B and A chains (the mature hormone) tethered by a flexible linker, producing rIAGs of the following commercially important species: Eastern spiny lobster *Sagmariasus verreauxi* (Sv), redclaw crayfish *Cherax quadricarinatus* (Cq) and giant freshwater prawn *Macrobrachium rosenbergii* (Mr). We then tested the biological activity of each, through the ability to increase phosphorylation in the testis; both Sv and Cq rIAGs significantly elevated phosphorylation specific to their species, and in a dose-dependent manner. Mr rIAG was tested on *Macrobrachium australiense* (Ma), eliciting a similar response. Moreover, using bioinformatics analyses of the *de novo* assembled spiny lobster transcriptome, we identified a spiny lobster tyrosine kinase insulin receptor (Sv-TKIR). We validated this discovery with a receptor activation assay in COS-7 cells expressing Sv-TKIR, using a reporter SRE-LUC system designed for RTKs, with each of the rIAG proteins acting as the activation ligand. Using recombinant proteins, we aim to develop specific tools to control sexual development through the administration of IAG within the critical sexual differentiation time window. The biologically active rIAGs generated might facilitate commercially feasible solutions for the long sought techniques for sex-change induction and monosex population culture in crustaceans and shed new light on the physiological mode of action of IAG in crustaceans.

1. Introduction

The androgenic gland (AG) was first identified in the male reproductive system of the blue crab *Callinectes sapidus* (Cronin, 1947). Since then, important milestone discoveries have established the key function of the AG in the development of masculinity of malacostracan crustaceans starting with pioneering work by Charniaux-Cotton (1954) followed by AG active protein fraction purification (Hasegawa et al., 1987), AG hormone isolation in isopods (Martin et al., 1990, 1999; Okuno et al., 1999), the first insulin-like gene (IAG) discovered in a commercially important

Abbreviations: IAG, insulin-like androgenic gland hormone; Sv, *Sagmariasus verreauxi*; Cq, *Cherax quadricarinatus*; Ma, *Macrobrachium australiense*; Mr, *Macrobrachium rosenbergii*; RTK, receptor tyrosine kinase; ILP, insulin-like peptide; GIH, gonad inhibiting hormone; MIH, molt-inhibiting hormone; RPKM, reads per kilobase per million.

* Corresponding author at: Faculty of Science, Health, Education and Engineering, GeneCology Research Centre, University of the Sunshine Coast, 4 Locked Bag, Maroochydore, Queensland 4558, Australia.
E-mail address: tventura@usc.edu.au (T. Ventura).

[1] These authors contributed equally to this work and should be considered co-first authors.

http://dx.doi.org/10.1016/j.ygcen.2016.02.013
0016-6480/

decapod (Manor et al., 2007) and the first successful silencing of a decapod IAG (Ventura et al., 2009), which eventually led to a commercial biotechnology to produce all-male populations; all of the above is extensively reviewed in (Ventura et al., 2011c; Ventura and Sagi, 2012). The AG was found to have a key regulatory role in crustacean male differentiation, including development and maintenance of the male secondary sexual characteristics and gonads. Microsurgical removal of the gland can result in complete sex-reversal, depending on the timing of intervention and the species involved. In other species, only the loss of external male sexual characters is observed (Suzuki and Yamasaki, 1991; Ventura et al., 2011c). Silencing of the IAG using RNA interference (RNAi) in the giant freshwater prawn *Macrobrachium rosenbergii* resulted in growth inhibition, followed by de-masculinization (Ventura et al., 2009). When applied within the correct developmental window (Ventura et al., 2011b), a fully functional sex shift was induced (Ventura et al., 2012), enabling monosex population culture (Lezer et al., 2015), validated through the use of sex markers to identify sex-changed individuals (Ventura et al., 2011a). In the Australian redclaw crayfish, *Cherax quadricarinatus*, IAG silencing in intersex individuals (which externally display both male and female gonopores and internally a testis on one side and an ovary on the other), resulted in reduced sperm production and testicular degradation accompanied by the onset of vitellogenesis to a level far exceeding that seen in untreated females (Rosen et al., 2010). This suggests that IAG has a role in regulating female secondary vitellogenesis, a hypothesis supported by the recent identification of IAG expression in late-vitellogenic stage ovaries in a crab species (Huang et al., 2014).

To better understand the function of IAG, several recombinant proteins have been produced and chemically-active proteins synthesized. To date, several expression systems were utilized to produce recombinant IAG (rIAG) proteins. Okuno et al. (2002) expressed a rIAG peptide of the woodlouse *Armadillidium vulgare*, in both baculovirus and bacterial systems. However, it was only after cleavage of the C-peptide that the protein (expressed in the Sf9 cells) was active *in vivo*, inducing masculinization of over 50% of injected females. Since the protein expressed in bacteria was not active, the researchers deduced that the N-glycosylation, previously identified by Martin et al. (1999), is vital for biological activity. Further studies in the woodlouse have also highlighted that correct disulfide pairing and consequential tertiary folding are also essential for biological activity of the mature protein (Katayama et al., 2010). Recently, Katayama et al. (2014) chemically synthesized IAG of the marine shrimp *Marsupenaeus japonicus* and tested the biological activity *in vitro* by culturing ovarian fragments from immature females with the recombinant hormone, causing a suppression in the expression of the vitellogenin gene. This result is consistent with the dramatic increase in vitellogenesis seen in *C. quadricarinatus* intersex individuals in response to IAG silencing (Rosen et al., 2010), as well as the peak in IAG expression seen in late vitellogenic ovaries of the mud crab, *Scylla paramamosain* (Huang et al., 2014), suggesting that IAG may also participate in inhibiting oocyte growth and vitellogenesis. While IAG has been characterized extensively, other components of the insulin signaling pathway remain predominantly unexplored in decapod crustaceans, as in other non-model invertebrates, mainly due to lack of genomic data (Boucher et al., 2010a) and the low number of known insulin receptors. In fact, IAG was the sole insulin-like peptide identified among the decapods, until the recent discovery of another insulin-like peptide (Sv-ILP1) in the spiny lobster *Sagmariasus verreauxi*, alongside insulin binding proteins (Chandler et al., 2015) and Sv-IAG (Ventura et al., 2015a), advancing our understanding of the insulin-signaling pathway in this commercially valued group of spiny lobsters.

Considering that IAG is a member of the insulin-like superfamily, we hypothesized that it would function through the conserved insulin-like pathway, involving an insulin receptor. However, to date, no such receptor has been identified in any of the Spiny lobsters. The insulin receptor is a transmembrane receptor that belongs to the ancient receptor tyrosine kinase (RTK) superfamily (Hubbard and Till, 2000). The insulin receptor is usually expressed as a single subunit that is then processed into two subunits, termed the α and β polypeptide chains, which are assembled into a heterodimer, or an $(\alpha\beta)_2$ homodimer that is stabilized by disulfide bonds (Maruyama, 2014). One of the most fundamental features of the RTK family is the downstream phosphorylation that occurs on ligand activation. Binding of the insulin-like peptide (ILP) ligand initiates a cascade of phosphorylation events, stimulating the downstream signal transduction and resulting cellular effect (Hubbard and Till, 2000). In the context of IAG, previous work by Khalaila et al. (2002), has shown that AG secretory products can directly activate protein kinases and phosphatases of some testicular polypeptides. This result provided the first evidence that the testis may possess testicular receptors that recognize AG secretory products. The postulation that the main secretory product of the AG is IAG has recently been reinforced through an in-depth transcriptomic analysis of the AG, which clearly shows that the hormone is a predominant secreted product of the AG. It therefore follows that IAG has been suggested to control the viability, proliferation and perhaps differentiation of sperm cells in the testes.

Over the last decade a large number of IAGs have been discovered and characterized, nevertheless protein characterization is still lagging. Native purification of the AG hormone is cumbersome, as it involves dissecting a large number of animals at a specific size and developmental stage, usually following eyestalk extirpation in order to remove the x-organ sinus gland complex, which regulates IAG production through inhibitory neurohormones (Khalaila et al., 2002; Sroyraya et al., 2010). More recently, these hormones were specifically identified as the gonad inhibiting hormone (GIH) and molt-inhibiting hormone (MIH), as shown by the negative regulation of the IAG gene in in *M. nipponense* (Li et al., 2015).

Recombinant hormones can be continually produced without the issues of animal availability to provide the source. The application of rIAGs can include studies of their specific structure, biochemical properties, receptor activation, production of antigens and *in vivo* administration for a biotechnological application. In the most commercially important group of penaeid shrimp, females grow faster and reach higher weights at harvest and thus all-female population culture will translate to increased productivity. This might be achieved through the application of rIAGs in order to produce 'neo-males'; phenotypic males with a female genotype that can be mated with females (Ventura and Sagi, 2012).

Herein, on the basis of the knowledge gathered so far, we identified, using bioinformatics analysis of the *de novo* assembled spiny lobster transcriptome, the spiny lobster tyrosine kinase insulin receptor (Sv-TKIR). We then validated this discovery using a receptor activation assay in COS-7 cells expressing Sv-TKIR, and a reporter SRE-LUC system designed for RTK. Activation was investigated using the synthesized rIAG proteins of three decapod species *S. verreauxi* (Sv), *C. quadricarinatus* (Cq) and *M. rosenbergii* (Mr), produced using the *Pichia pastoris* yeast system, thus validating both receptor activation and the biological activity of our recombinant proteins. We further examined the biological activity of the rIAGs using a phosphorylation *in vitro* assay. To our knowledge this is the first characterization of an insulin receptor in decapods, where activation has been proven through the use of rIAGs.

2. Material and methods

2.1. Animals

Redclaw crayfish, *C. quadricarinatus* (Cq) live males weighing 107–127 g, were purchased locally from Cherax Park Aquaculture and were grown and maintained in closed re-circulatory systems of 200 L tanks. Temperature was kept at 27 °C ± 2, and the total water volume of the system was kept recirculating through a bio-filter. A photoperiod of 14L: 10D was applied. Food pellets were supplied *ad libitum*. A live male spiny lobster *S. verreauxi* (Sv) male weighing 2.5 kg and 50 live male freshwater prawns, *Macrobrachium australiense* (Ma) weighing 0.53–4.08 g were purchased locally. Prior to dissections, animals were anesthetized on ice for at least 20 min.

2.2. Recombinant IAGs production

Synthetic IAG genes were ordered from GeneScript (Piscataway, USA). The genes contained a linker containing a His-tag and the codon usage was optimized to the codon bias of *P. pastoris* to facilitate higher expression rates. All recombinant proteins used in this work were cloned into the *EcoRI-NotI* sites of the pPIC9K expression vector. Briefly, the mature protein-coding sequences (B and A chains; GenBank Accession No. Sv: AHY99679.1, Cq: ABH07705.1, Mr: ACJ38227.1) were joined to form a fusion gene that encodes a "tethered" polypeptide in which the B chain forms the N-terminal and the A chain forms the C-terminal. A "linker" sequence of amino acids (GSGSHHHHHHHGSGS) was placed between the B chain and the A chain to assist in the chimerization of the subunits, with the six-His tail placed in the middle of the linker to enable purification of the recombinant protein (Fig. 1A). The recombinant single chains were sub-cloned into pPIC9K expression vector. Prior to yeast transformation, the pPIC9K vector containing the synthetic gene was linearized with *Sal I* to obtain Mut+ (methanol utilization plus: refers to the wild-type strains' ability to metabolize methanol as sole carbon source) transformants. The *Sal I*-linearized expression cassette was then transformed into the host *P. pastoris* SuperMan5 strain (his$^-$), a GS115 (his4-) variant with the alpha 1,2-mannosidase from *Trichoderma reesei* regulated by the GAP promoter on a plasmid with the blasticidin resistance gene disrupting the Och1 gene in the SuperMan5 genome, by electroporation. This resulted in insertion of the construct at the AOX1 locus of *P. pastoris*, generating a His$^+$ Mut$^+$ phenotype. 100 Mut+ transformant colonies were screened by resistance test with 0.5–2 mg/ml antibiotic (G418 geneticin). Ten His/Mut+ clones were chosen and cultured for small scale production in a shaker flask for 1 day (growth phase) in BMG at 28 °C. Cells were harvested by centrifugation, resuspended and cultivated for 3 days (induction phase) in BMM medium. The proteins were expressed in a shaker flask and harvested after induction by methanol. Recombinant proteins were purified using nickel-nitrilotriacetic acid-agarose (Ni-NTA; Qiagen). Using the methylotrophic yeast *P. pastoris*, rSv-IAG, rCq-IAG and rMr-IAG were produced as biologically active, single-chain polypeptides according to Aizen et al. (2007) by using the *Pichia* Expression kit (Life Technologies Corp.).

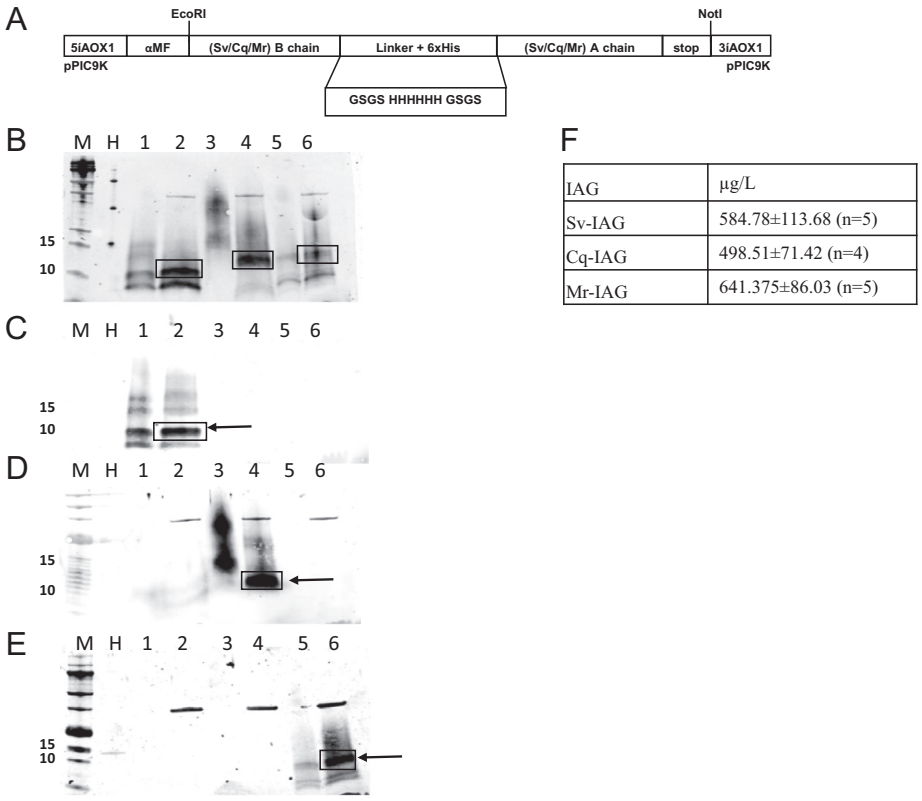

F

IAG	µg/L
Sv-IAG	584.78±113.68 (n=5)
Cq-IAG	498.51±71.42 (n=4)
Mr-IAG	641.375±86.03 (n=5)

Fig. 1. Characterization of *P. pastoris*-expressed rIAG by Western blot analysis. (A) Schematic representation of the expression cassette in pPIC9K vector for each IAG. (B–E) Proteins from *P. pastoris* cultures were separated on a 16% Tricine Gel, and were immune-reacted with anti His-Tag (B), anti Sv-IAG (C), anti Cq-IAG (D) or anti Mr-IAG (E). Lanes 1–6 were loaded with 15 µl, from a culture of 1 L that was nickel batch purified (even lane numbers included deglycosylation): rSv-IAG (lanes 1 and 2), rCq-IAG (lanes 3 and 4) and rMr-IAG (lanes 5 and 6). M indicates molecular marker and expected molecular weight is indicated by a black box and an arrow. (F) 1 L production summary for each rIAG, data is presented as Mean ± SEM, µg/L.

2.3. Western blot analysis

Reduced or nickel-purified samples, both non-deglycosylated and deglycosylated (by PNGase F (New England Biolabs) from culture supernatants) were electrophoresed on 16% Tris/Tricine gels. Gels were blotted onto nitrocellulose membranes using Trans-Blot Turbo Transfer System (Bio-Rad) and blocked with 3% BSA in TBS-T. Recombinant IAGs were visualized with an antibody against the His-tag (QIAexpress anti-His antibodies; Qiagen). When using the anti-His antibody, the membranes were treated according to the manufacturer's recommendations (1:2000 dilution). Membranes were next incubated with IRDye® 800CW Goat anti-Mouse secondary antibody for 1 h at room temperature. When specific antibodies i.e. Sv-IAG (produced by Genescript), Cq-IAG and Mr-IAG (received from Prof. A. Sagi) were used, the membranes were blocked with 5% skimmed milk in TBS-T and incubated in 1% skim-milk in TBS-T with the antibodies (1:1,000 dilution) overnight at 4 °C. Membranes were next incubated with IRDye® 680CW Goat anti-Rabbit secondary antibody for 1 h at room temperature. After washing, all membranes were analyzed using an Odyssey Infrared Imaging System (LI-COR Biosciences).

2.4. Sv-TKIR transcriptomic assembly and validation

In order to identify the putative *S. verreauxi* TKIR, tblastn analyses were run against the entire *S. verreauxi* transcriptome (Chandler et al., 2016, 2015; Ventura et al., 2014, 2015b) using orthologs from *D. pulex* (Accession number: EFX63421.1 aka Dp-InR3) and *D. melanogaster* (Accession number: AAF55903.2) and CLC (Main Workbench v 7.0). A complete transcript was not identified using either ortholog, only transcript fragments correlating to the full TKIR. Therefore, "*in silico* RACE" techniques were used to assemble a full transcript. This involved alternatively blasting each orthologous transcript fragment against two different assemblies of the *S. verreauxi* transcriptome (BGI and Trinity assemblies). This enabled the identification of all transcript fragments of identical, overlapping 5′ and 3′ termini, thus assembling a full gene transcript. Of the two reference insulin receptors, the *D. melanogaster* IR (Dm-IR) but not the *D. pulex* (Dp-InR3), facilitated the assembly of a complete *S. verreauxi TKIR* transcript; the receptor was named *Sv-TKIR* (GenBank accession number: KT163378). The *in silico* assembled *Sv-TKIR* was then validated by RT-PCR. Due to the restraints of Sanger Sequencing, the 7081 nt transcript was divided into seven, ~1000 nt sections, using consecutive, flanking primers to ensure complete coverage; Table S1 details primers with associated sequence positions. RT-PCR validation was conducted as described in Chandler et al. (2015), with the amended elongation time of 1 min per cycle and final extension of 15 min. PCR products were then excised from the gel and DNA extracted using the QIAquick Gel Extraction Kit, QIAGEN, following manufacturer's instructions. Sanger sequencing was conducted by AGRF, Brisbane. Sequenced gene fragments aligned identically with the *in silico* assembled *Sv-TKIR*, fully validating the *in silico* assembly and open reading frame (ORF) of the sequence. Additionally, RT-PCR using a range of primer combinations, amplifying overlapping segments up to ~3000 nt gave repeatable, amplified coverage of the entire transcript, fully validating the sequence. The receptor then was sub-cloned into pcDNA3.1 plasmid for further analysis according to previously described procedures (Shpilman et al., 2014).

2.5. Phylogenetic analyses of Sv-TKIR

Phylogenetic analyses were conducted with a range of the top orthologs collected from the Blast output of Sv-TKIR at NCBI, as well as additional model species for phylogenetic diversity. The sequences were aligned using CLC Workbench (7.5.1) and a Neighbor-joining tree was constructed; bootstrap analyses of 1000 replicates were carried out to determine confidence of branch positions. Bootstrap values of >75% were highlighted in bold to indicate confidence of positioning. For a full table of species and associated Accession Numbers see Table S2.

2.6. Spatial expression analyses of Sv-TKIR

Expression was analyzed both digitally and using RT-PCR. Initially expression was quantified using the digital gene expression measure of reads per kilobase per million reads (RPKM) based on transcriptomic data. As the full gene sequence for *Sv-TKIR* was present as several transcript fragments, each of which has its own associated RPKM, all of these fragments (which together assembled the full *Sv-TKIR*) were collated and an average RPKM value across all fragments calculated. The standard error was also calculated to demonstrate the consistency of RPKM values across transcript fragments. Transcriptomic tissue libraries included male and female brain (BR), eyestalk (ES), gonads (TS and OV), antennal gland (AnG), fifth walking leg (5WL) and the mature androgenic glands (AG77 and AG36; note that AG36 was a hypertrophied gland, mediated *via* eyestalk ablation; unpublished data). To validate this digital expression profile, we undertook a spatial expression analyses using RT-PCR with Primer Set 1 (see Table S1). RNA was extracted from those tissues described above, as well as from male and female hepatopancreas (HP) and cDNA was prepared as described in Chandler et al. (2015); a 16S positive control was run under identical conditions; both ran a negative control in the fifteenth lane. Amplicons were then electrophoresed on a 1.5% agarose gel stained with ethidium bromide and visualized under UV light.

2.7. Cell culture and transient transfection of cells

Transient transfection, cell procedures and stimulation protocols were generally according to Aizen et al. (2012). COS-7 cells were purchased from European collection of cell Cultures (ECACC). Briefly, COS-7 cells were grown in DMEM supplemented with 10% FBS, 2 mM L-glutamine, 100 U/ml penicillin, 100 mg/ml streptomycin and 100 U/ml Nystatin (Life Technologies) under 37 °C, 5% CO_2 until confluent. Co-transfection of the *Sv-TKIR* (at 7.5 μg/plate) and a SRE-LUC (pGL4.33[luc2P/SRE/Hygro], Promega) reporter plasmid (at 7.5 μg/plate) was carried out with TransIT®-LT1 Transfection Reagent (Mirus), according to manufacturer's instructions. The cells were serum starved for 24 h, stimulated for 6 h with rCq-IAG, rSv-IAG or rMr-IAG and human insulin, and then harvested. Lysates prepared from the harvested cells were assayed for luciferase activity and experiments were repeated a minimum of three times from independent transfections, each performed in triplicates. COS-7 cells were transfected with empty pcDNA3.1 as a negative control and showed no changes in luciferase activity in all experimental groups (data not shown). To compare the biological activities of the different IAGs, half-maximal effective concentrations (EC50) were calculated using Prism software and compared.

2.8. In vitro bioassay

Briefly, testes from six mature *C. quadricarinatus* males (Cq; mean ± SEM, 117.5 ± 9.8 g of body weight [BW]); gonadosomatic index [GSI] [i.e., gonadal weight percentage of BW], 0.65% ± 0.34%), one *S. verreauxi* (Sv; 2.5 kg; GSI = 0.08%) and fifty *M. australiense* (Ma; mean ± SEM, 1.08 ± 0.48 g; the small animal size did not enable accurate GSI calculation) were divided into uniformly sized fragments (of about 25–30 mg each). The fragments

were washed 3 times for 5 min in a 24-well culture plate at 28 °C in the presence of Leibovitz's L-15 Medium (Sigma). The testis fragments were then rinsed and the medium was replaced with the same medium with or without the rIAG to be tested. Stimulation with each IAG, at graded doses (500, 50 and 10 ng/ml), was continued for 15–20 min. These incubations were performed in triplicate wells per treatment. Testis fragments were collected for total protein purification as described in Section 2.9.

2.9. Mapk1/2 phosphorylation

Following the *in vitro* bioassay the L-15 medium was removed and 150 µl of RIPA buffer (Cell Signaling) containing Protease Inhibitor Cocktail Set III (Calbiochem) was added, followed by homogenization and centrifugation to obtain a lysate fraction as described previously by Aizen and Thomas (2015). Lysates (30 µg/lane) were loaded and run on 10% Tris-Glycine gels, the proteins transferred to nitrocellulose membranes, and Western blot analyses conducted as described previously. Membranes were probed with antibodies for phospho-p44/42 Mapk (Erk1/2; Cell Signaling #4370) and total p44/42 Mapk (Erk1/2; Cell Signaling #4695) and Image J software was used to quantify the protein bands.

2.10. Statistical analysis

Data are presented as the mean ± SEM. One-way ANOVA determined the significance of differences between control and treatments with Bonferroni multiple-comparison test using GraphPad Prism 6.05 software (GraphPad Software).

3. Results

3.1. Production of recombinant IAGs

Following the selection of the super clone that showed the highest expression, a production of a large-scale (1L) of rSv-IAG, rCq-IAG and rMr-IAG was performed. The yield of the different IAGs varied between 498 µg/L and 641 µg/L (Fig. 1F). Western blot analysis of the rIAGs yielded bands of 10 to 15 kDa at the expected sizes of the recombinant proteins (rSv-IAG – 9.36 kDa, rCq-IAG – 11.23 kDa and rMr-IAG – 11.49 kDa). The samples were further analyzed for specific molecular weight by de-glycosylation of the recombinant proteins (Fig. 1B, lanes 2, 4, and 6) when immunoreacted with an antibody against the His-tag (Fig. 1B). Under reducing conditions, the immunoreactive rSv-IAG, rCq-IAG and rMr-IAG revealed bands of about 10, 11 and 12 kDa, respectively (Fig. 1B, lane 2, 4 and 6). When tested with their specific IAG antibody each protein specifically bound its cognate antibody and had the expected size (Fig. 1C–E, lane 2, 4 and 6). Transformation with the vector alone (i.e., GS115/pPIC9K [Mut$^+$]), serving as a negative control, showed no bands when immunoblotted (data not shown).

3.2. TK receptor

3.3.1. Sv-TKIR

The entire, assembled *Sv-TKIR* transcript was 7081 nt in length, corresponding to an ORF of 6018 nt, start codon at 815 nt and stop codon terminating at 6832 nt (with a 814 nt untranslated 5′ region and a 249 nt untranslated 3′ region). When translated, the 6018 nt ORF generated a 2005 amino acid (aa) sequence, termed Sv-TKIR. Sv-TKIR shows all the conserved domains expected of an RTK, with no evidence of truncation: namely the presence of the signal peptide (from 1 to 34 aa), the receptor L domains (from 255 to 370 aa and 547 to 659 aa) which form the bilobal external ligand binding site, containing a region of furin-like repeats (from 428 to 471 aa), three fibronectin type 3 domains (from 681 to 780 aa, 796 to 1081 aa and 1118 to 1198 aa), the transmembrane domain (from 1219 to 1241 aa) and the internal tyrosine kinase catalytic domain (from 1286 to 1542 aa); Fig 2A and B. Regions of low complexity are also found at the N and C-terminal. The C-terminal shows an extended region of 463 aa post the terminal tyrosine kinase domain, an extension also noted in the insulin receptor of *D. melanogaster*.

3.3. Phylogeny

The *S. verreauxi* TKIR (placed with a bootstrap confidence of 45%) shows closest similarity with the platyheliminths, *Echinococcus granulosus* (placed with a confidence of 100%), and the two insulin receptors from *Schistosoma mansoni* (placed with bootstrap values of 87% and 100% respectively) (Fig. 2C). The same branch also includes the arthropod *Zootermopsis nevadensis* (a dampwood termite) although, similarly to *S. verreauxi*, this branch is placed with a lower bootstrap value than that of the platyheliminths (57%). The co-joining branch includes the cnidarian, *Hydra vulgaris* as the species showing closest similarity to *S. verreauxi*, separated from the Chordates by the echinoderm, *Strongylocentrotus purpuratus* and the hemicordate *Saccoglossus kowalevskii*. The chordates form a confidently placed cluster showing branching within their respective orders. With regard to the other members of arthropoda, *Bombyx mori* also shows divergence from the main arthropod group (similar to *S. verreauxi* and *Z. nevadensis*), branching closer to the nematode *Caenorhabditis elegans*. All remaining members of athropoda, including *Daphnia pulex*, as a member of the crustacea, cluster within their Phyla, the majority of which are placed with a confidence >75%. The molluscs form another confidently placed sub-group, branching in between the primary cluster of arthropoda and the chordates.

3.4. Expression of Sv-TKIR

The spatial expression of *Sv-TKIR* was quantified through the digital measure of RPKM, with supporting RT-PCR analyses. There is strong correlation between both digital and molecular methods which clearly indicate that *Sv-TKIR* shows predominant expression in the male testis (TS) and both male and female antennal glands (AnG), where in fact the female AnG shows higher expression than that seen in the male. With regard to the RT-PCR profile, there is an indication of expression in the hypertrophied AG36, with evidence of a very faint band. All other tissues appear to show basal expression levels (Fig. 3). This corroboration of digital and molecular expression profiles is good evidence for the accuracy of our RPKM quantification and overall transcriptome assembly.

3.5. Receptor activation

In order to test the biological activity of the rIAGs we used the Serum response element (SRE) reporter. rSv-IAG stimulated SRE-LUC activity in COS-7 cells expressing Sv-TKIR in a dose-responsive manner, with levels of EC_{50} = 10.54 ± 0.60 ng/ml. Interestingly the human insulin (h-Insulin, Sigma) also elicited a response, although with higher EC_{50} levels of 94.56 ± 0.61 ng/ml. rCq-IAG did not elicit any response in the measured concentrations and rMr-IAG was only slightly effective at a very high dose (Fig. 4).

3.6. Phosphorylation in vitro assay

The ability of IAG to activate phosphorylation events has previously been shown using AG gland extract, suggesting phosphorylation is involved in IAG signaling (Khalaila et al., 2002). Our work has shown that treatment with rIAGs for 15–20 min resulted in

(A)

```
01   MVFHITPIVVVSVTGVYVTCRLVVARVSYLQVNTFLDLYPFSCLQESQGLTAWCGSSKHSK
62   HHLLNEHKQFMYNVENDRYMKIFQIVSAKLYDQSKLKMKECETRTKASIRILQKSQRKSVR
123  TPMILNPKERVELLSHSDKRLELRSEEVSESLDGTRKTVSPSLSQCIRREDTTASPVPTPG
184  TRPFRGTSWGVGRWWKVVVVLALWVWAGECRAQASTHHTPNICQQRYNGTADKICGSMDLR
245  NSISALEKLCPCRIIDGHLHFVLQEQRDSASMTRLSQYSFPGLREITHHLLIYRVFSLASL
306  HSLFPNLAVIRGDVLFHNYALVIYDVPSLQEVGLVSLTVILRGSVRIERNPQLCYVHTVDW
367  GHITVNRLAENYINRNRPVSECPSCPEELGCRRSKGCGAPRCWGSHACQSRCGSECPGGCV
428  GDQCCHEECLGGCLTPGDPNTCHACRSLLDDGRCTHACSSPKFKVLKHRCETREVCSSQYA
489  IKRDTQECVERCPLGYNETVTRMGSRNVTECVPCEGYVCTKQCSARTVKSISHAQLLRGCT
550  EIDGHLTVHINGGENIEQELVENLSGIEVVRSYVKIFRSNITSLNFLSNLTTIGGSQLLYS
611  NYSLVILDNPNLQTLWNTTNLTIKKGKVFVQSNPKLCLHHVQELINNTNITGLSDTDVSST
672  SNGDKVPCKVTPLKASVSTSVLYGTLTVTVFPHLPSVTVYYVNYKKADRNISLYESEGPCS
733  DQGWSTVEMAAGNATGAGGAVHGTIVNLEPYTRYAVYVKTYSLASSEEGAQSDVLYAVTSP
794  YNPTEPVHLEWASPNSRTLELWWEAPRRPNGQIDHYLVKLTLLPDTPRIPPDFDFCSPETR
855  KYVDKKMAAMAQAEATIAPVRKTPTVEQKDPAEDPGGDDLCQATPATPSCCACRHPRLDED
916  HEVMGQISFEDFIMDNVYVKKINRSGRRTRESRLISDEEFENKLQAAHHPHTRNTLLKTVQ
977  SNASTSFGEADGEDDLSVSSFEDEDFPVHWGQTVHEFPTHAGIEADYRLHEENLTEYDRPH
1038 PNLSSVLLEQVHMTREPRLTLDNLHHFSLYSVGVVACQAPLGVSVSDQWGQPSPQGKLCST
1099 IPARTAAYTRASDAADLIPEGSLRTMVLNNTSKESVVITWDPPGSPNGGVVAYILKIQSFS
1160 RDRCINSREFEYQGRRVEVRDLSPGNYSVWVKVRSKAKYGNVSAPAYFIIKDASRTDVSLV
1221 VASSLLAVAGAVLAAFTYWLWRRFRLTYSIPDTLDKVDINPYYREGFAPAEIFREEFIFWR
1282 DDLKVFYDRPLGQGFFGMVFEGQLNKDSRRTRVAVKTHSERATNEEIGQFLKEAAVVQNIS
1343 CHHVVRLLGVVGDYAPVYVVMELMQEGDLKTFLNKHPPNFITGQKMMEMAVEAADGMAYLA
1404 AGKLVHRDLAARNCMLDHQLTLKIGDFGLTRNLKSDYYRTGGQGAMPVKWMAPESLQFNLY
1465 STQSDVWSYGVLLWEMATRGVTPYKNRTNDEVIRLVVERYATPGRPKNCPLPIQRLMRCCW
1526 RYEARERPTFIAITKYLLKYTSLDYQKRFEQVSFYHSRSSDYSKYQRKETCGFMSECARES
1587 EEDLDQLALLTSCEASEEDISERDSGRYRSTPHGSPRLGRGSSPRLRKMSPRPSTTSFGRT
1648 LDGGDGLQCDHSQHSSPGDLRQEEKIKRHLYSNFDSEELHFGQRLQAGGASQMAPPGGLPT
1709 LLIPQDYRELRYAQLQLSTPSTPASGSHTPSSCPLTPSSNPQTPFLHPHSGLWPSPTCPSL
1770 QRSVSPLALNSPGSSPTLLNSSQTSVKSRASSPKLMRALYSNLQCLSSLQVASSTLALSPT
1831 PLNVGSRPPLNTPTQRSATEEPSRRFTGERCLAATTASTPAIPHGSEQPHRHMSKSTIHSP
1892 STRDPPIPAPGPGVNPRHPQWPCNPPPSSSATPTTSSPLEAEHAHVHSSSCPAVSQDSSRQ
1953 DLGSCSGSLHRWIQKVSPPASLPRSRSGPLRKKAASEGQMQKDSSPPGAFEIL*
```

(B)

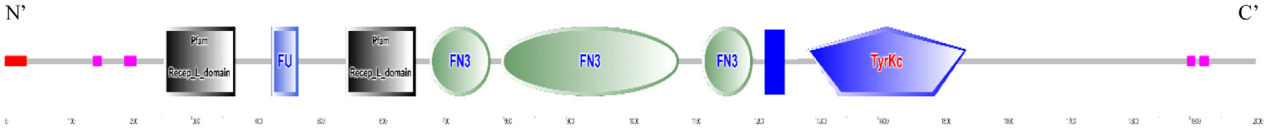

(C)

Classification	Species
Cnidaria	*Hydra vulgaris*
Nematoda	*Caenorhabditis elegans*
Platyheliminths	*Schistosoma mansoni*-IR1, IR2
	Echinococcus granulosus
Hemicordata	*Saccoglossus kowalevskii*
Echinodermata	*Strongylocentrotus purpuratus*
Mollusca	*Pinctada fucata*
	Crassostrea gigas
	Aplysia californica
Athropoda: Chelicerata	*Ixodes scapularis*
Crustacea	*Daphnia pulex*- InR1, 2, 3, 4
	Sagmariasus verreauxi
Isoptera	*Zootermopsis nevadensis*
Hemiptera	*Acyrthosiphon pisum*
	Nilaparvata lugens
Coleoptera	*Tribolium castaneum*
Hymenoptera	*Apis mellifera*
	Bombus terrestris
	Camponotus floridanus
	Solenopsis invicta
Lepidoptera	*Bombyx mori*
Diptera	*Drosophila melanogaster*
Chordata: Cypriniformes	*Danio rerio*- IRa, IRb
Amphibia	*Xenopus laevis*
Aves	*Haliaeetus leucocephalus*
Rodentia	*Mus musculus*
	Rattus norvegicus
Primates	*Macaca mulatta*
	Homo sapiens

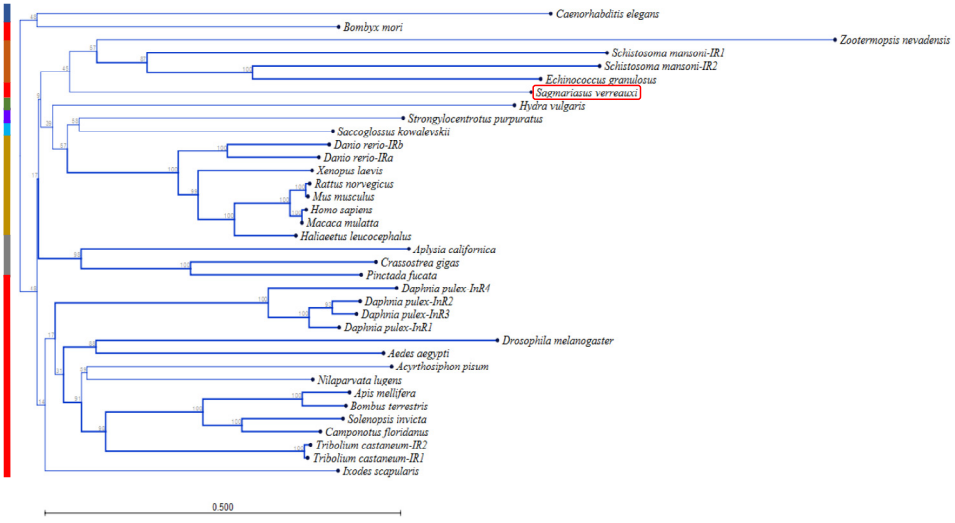

Fig. 2. Sv-TKIR: the *S. verreauxi* tyrosine kinase insulin receptor ortholog. (A) The translated ORF of *Sv-TKIR*, giving the amino acid sequence of Sv-TKIR from N-terminal to C-terminal: signal peptide shown in red, followed by two receptor L domains highlighted in dark grey which together form the bilobal external ligand binding site, separated by the region of furin-like repeats highlighted in blue. The three fibronectin type 3 domains are shown in green followed by the transmembrane domain and the internal tyrosine kinase catalytic domain at the C-terminal. Asterix marks the stop codon. (B) Smart domain architecture of Sv-TKIR, shown in identical colors and orientation to that described in A: *Recep_L_domain* indicates the receptor L domains; *FU*, the furin-like repeats; *FN3*, the three fibronectin type 3 domains; the blue rectangle depicts the transmembrane domain; and *TyrKc*, the tyrosine kinase catalytic domain. Regions of low-complexity at the N-termianl and C-terminal termini are indicated by pink boxes. (C) Phylogenetic analyses of insulin-like receptors across Animalia. Phyla are indicated by color as indicated in the key; members of Arthropoda are highlighted in red. Please refer to classification table for more specific classifications of the Orders of *insecta* and *chordata*, which are listed in the context of decreasing evolutionary time from the most ancient. Bootstrap values are shown at each node and those values $\geqslant$75% are highlighted in bold, Bootstraps were performed with 1000 replicates to ensure reliability.

increased Mapk1/2 phosphorylation in testicular fragments, confirming the previous findings of (Khalaila et al., 2002). In Sv testicular fragments, phosphorylation of Mapk2/1 in response to rSv-IAG was increased when 500 ng/ml was applied, demonstrating that activation of Mapk2/1 involves Sv-IAG (Fig. 5A). Both rMr-IAG and rCq-IAG had no effect on the phosphorylation in the Sv testicular tissues compared to the control group. The phosphorylation of Cq testicular fragments increased at all doses of rCq-IAG but only the higher dose was significant and reached 4-fold higher phosphorylation than the control group. Both rMr-IAG and rSv-IAG had no effect. Interestingly, the activation of Ma testicular fragments by rMr-IAG was low in the higher dose (500 ng/ml) and high at lower doses (10, 100 ng/ml). Both rSv-IAG and rCq-IAG had no effect compared to the control group (Fig. 5). In summary, all three

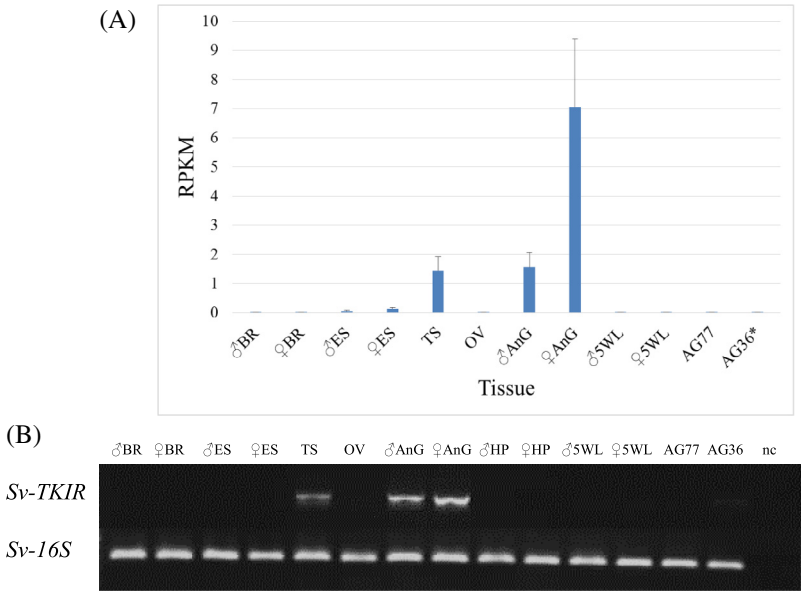

Fig. 3. Spatial expression analyses of *Sv-TKIR*. (A) The transcriptomic expression profile of *Sv-TKIR* quantified through digital gene expression, as reads per kilobase per million reads (RPKM). As the full gene was present in transcript fragments, an average RPKM has been taken from across all transcript fragments that assemble to give the full *Sv-TKIR*; error bars indicate the standard error of this average. Expression is shown across all transcript libraries, namely the male and female brain (BR), eyestalk (ES), gonads (TS and OV), antennal gland (AnG) and fifth walking leg (5WL) and the mature androgenic glands (AG77 and AG36, where * indicates that AG36 was a hypertrophied gland). (B) The RT-PCR expression profile of *Sv-TKIR* (using primer set 1, see Table S1) including all the tissues used for transcriptomic analyses with the addition of male and female hepatopancreas (HP) to give a thorough spatial expression profile; both expression profiles show strong correlation. Negative control (nc) in the fifteenth lane, with 16S acting as a positive control.

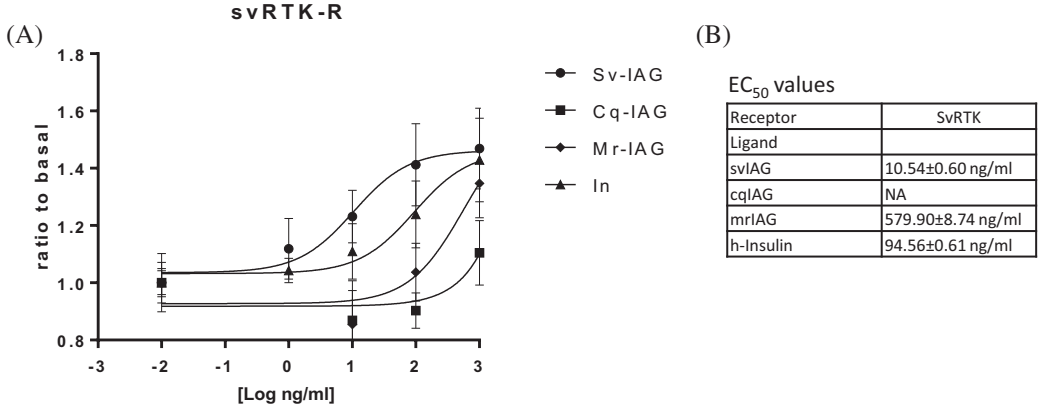

Fig. 4. Sv-TKIR activation in COS-7 cells. Sv-TKIR stimulates SRE-LUC activity. (A) COS-7 cells were transiently co-transfected with Sv-TKIR and the reporter plasmid pSRE-LUC. Cells were stimulated for 6 h with each rIAG (Sv, Cq or Mr) and human Insulin at different concentrations. Luciferase activity was determined, and results are presented as ratio to basal. (B) Summary of EC50 values for the each rIAG used in this study in COS-7 cells. Data are presented as mean ± SEM ($n = 3$) in ng/ml of a representative experiment that was performed in triplicate. Conversion to molarity is presented in Supplementary Fig. 4.

rIAGs produced increased testicular phosphorylation in a dose- and a species-specific manner.

4. Discussion

The present study provides clear evidence that the IAG hormone is regulating phosphorylation through a tyrosine kinase insulin receptor. Although previous studies have shown the involvement of AG in the phosphorylation of testicular polypeptides (Khalaila et al., 2002), direct evidence was lacking. Using a synergy between advanced bioinformatics and biotechnology methods, we were able to identify the insulin receptor in *S. verreauxi,* activate it with rIAGs in a dose response manner and show that the hormone shows species-specific activation among three decapod species. Although it has long been known that IAG is the hormone that governs male sexual differentiation in malacostraca (Ventura et al., 2011b), there has been minimal understanding or demonstration of the biological pathways that facilitate the hormone's masculinizing effect.

Our research describes the identification of a tyrosine kinase insulin-receptor in *S. verreauxi* (Sv-TKIR) which shows all of the conserved functional domains of the RTK superfamily. Sv-TKIR has an extended C-terminal, similar to that found in *D. melanogaster* and may explain why the *D. melanogaster* sequence enabled the assembly of the full *S. verreauxi* sequence, unlike the closer relative, *D. pulex*. The lack of similarity between Sv-TKIR and the *D. pulex* IR is most likely a reflection of the variable nature of the IR in *D. pulex*, with the species expressing four distinct IR (InR1-4) each of which shows a distinct domain architecture and all of which have a truncated C-terminal (Boucher et al., 2010b).

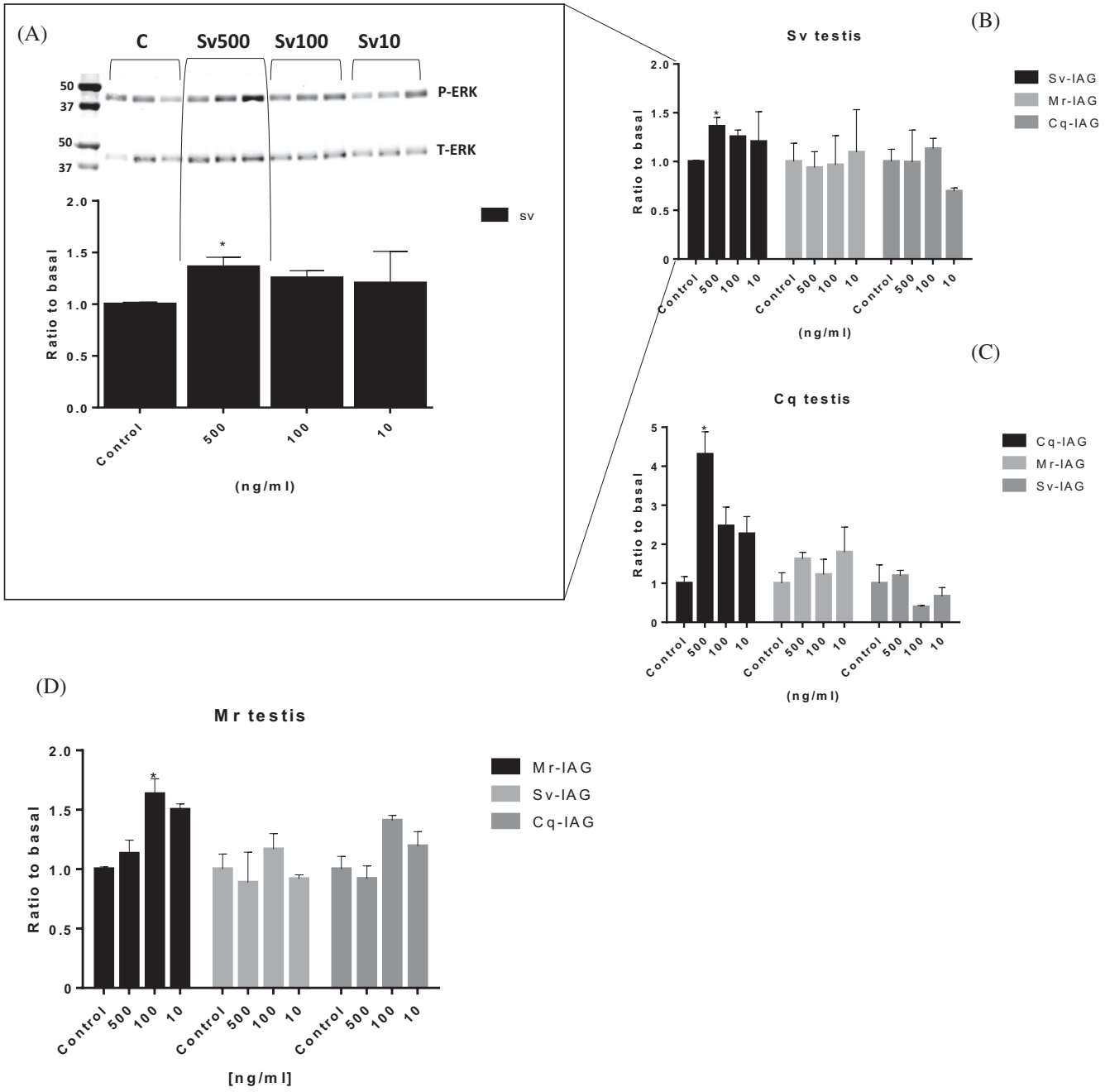

Fig. 5. Effects of 15 min treatment with rIAGs (10, 100 and 500 ng/ml) on phosphorylation of Mapk1/2 in Sv, Cq and Ma testicular fragments by Western blot analysis. P-Mk2/1, phosphorylated Mapk1/2; T-Mk1/2, total Mapk1/2. Testicular fragments were treated for 15 min with the rIAG and phosphorylation level was measured by western blot. Representative western blot are shown. Relative amounts of P-Mk2/1 compared with their loading controls, T-Mk1/2, determined from densitometry of western blots. All of the Western blots are shown in supplementary Figs. S1–3. Conversion to molarity is presented in Supplementary Fig. 4.

Considering the broader phylogenetics of the IR (Fig. 2C) our phylogeny shows clear evolutionary clustering, with those most ancient species (including *S. verreauxi*) showing similarity, while their recently evolved counterparts in the insecta present as clearly phylogenetically distinct, as does the separate lineage of the chordates. This phylogeny is clear evidence of the early emergence and conservation of the TKIR, evidence of a fundamental role across a diversity of phyla. Although well conserved, there is divergence seen in the number of TKIRs found among species. Considering the invertebrates studied to date, it appears that only one homolog of the IR gene tends to exist (Boucher et al., 2010b), with *Schistosoma mansoni* (Khayath et al., 2007), *Tribolium castaneum* and *D. pulex*, presenting as the anomalies, seeming to be resultant from species-specific duplication events and divergence (Fig. 2C) It is only in the vertebrates where duplication events have been conserved, resulting in three IR paralogs, where sub-functionalization has enabled each to evolve a specific function in co-evolution with ligand diversification (the insulin receptor, IR (displayed in Fig. 2C); as well as the IGF1 receptor, IGF1R; and the insulin related receptor, IRR) (Hubbard and Till, 2000).

It seems that *S. verreauxi* conforms to the norm of the invertebrates, with a single IR. This suggests that all expressed insulin-like peptides (ILPs) in *S. vereauxi*, including Sv-ILP1 (Chandler et al., 2015) and Sv-IAG (Ventura et al., 2015a), will have some

functionality through Sv-TKIR. However, previous work in *Aedes aegypti* (Wen et al., 2010) has shown that ILPs tend to show differential binding affinity for the single IR, with some perhaps showing preferential binding-activity through distinct receptors, such as a G-protein coupled receptor (Veenstra et al., 2012), which we hypothesize to be the case for Sv-ILP1 (being an ortholog of Dilp7). Interestingly, although not a complete homolog, an incomplete decoy IR has been noted in *Drosophila* (Okamoto et al., 2013), acting as a sink (or negative regulator) for ILP signaling. The decoy contains only the extra-cellular components of the IR, with none of the C-terminal internal catalytic domains necessary to induce signal transduction. Indeed, we were able to identify a similar decoy TKIR in *S. verreauxi*, consisting of a truncated C-terminal peptide lacking the third fibronectin, transmembrane and TK catalytic domains. This suggests that a similar mode for the negative regulation of ILPs may function in *S. verreauxi*. *Sv-TKIR*-decoy RPKM expression is limited to the ovary (OV) and mature AGs (AG77 and AG36; data not shown), both represent tissues which require temporally-regulated sensitivity to IAG at particular maturation states (cessation of secondary vitellogenesis or inhibition thereof in immature females, as discussed previously, and stimulation of AG proliferation in immature males). It may be the case that here, in the mature individuals used in this study, these IAG-mediated effects are no longer required, hence the decoy is expressed as a sink for IAG, preventing its downstream effects within the cell.

The use of biotechnology to produce an active AG hormone has been implemented previously, through the use of both baculovirus and bacterial expression systems (Okuno et al., 2002). In both systems the C-peptide had to be cleaved in order to render the protein biologically active. Furthermore, the separation process involved HPLC, making the production process cumbersome and prone to a loss in protein quantity during the cleavage and following recovery procedures. Recently, Katayama et al. (2014) expressed the IAG hormone using a chemical synthesis method. Compared to other expression systems, the yeast system used in this study can overcome the production of single-chain or proinsulin that needs to be cleaved in order to become the active hormone. We have overcome this caveat by using a flexible linker connecting the two chains, to comprise the mature, active hormone. In this study we use repeats of glycine and serine in order to allow the A and B-chains to refold and orientate correctly. The use of glycine-serine linkers has been described and used extensively in different species with a variety of proteins (Reddy Chichili et al., 2013). Studies with single-chain insulins have shown that the length of the linker should be 9–15 amino acids in order to enable proper folding and result with receptor activation (Rajpal et al., 2009). We employed a linker within these boundaries (14 aa), with a histidine tag embedded in the middle (Fig. 1A), in order to facilitate the specific purification of our desired hormone from the medium in which it was secreted by the yeast.

Okuno et al. (2002) produced the first IAG recombinant hormone in two different production systems; in Sf9 cells the yield was 5 μg/ml and in bacteria 1 μg/ml. These concentrations correspond to the pro-hormone, which still includes the C-peptide, and could account for half the molecular weight. In these expression systems insulin-like proteins need to be cleaved in order to serve as active hormones. Since there is no data on cleaved protein recovery rate, the final yield can be considerably reduced. In our study we produced an average of 0.57 μg/ml using the yeast system, employing 1 L shaker flasks. This procedure can be directly upgraded to fermentation using a bioreactor, where previous human insulin production has yielded 15–36 μg/ml (Gurramkonda et al., 2010; Wang et al., 2001; Xie et al., 2008) using the same *P. pastoris* system that was used in this study.

In the current study using His-tag antibodies, western blot bands demonstrated that each rIAG corresponded with its expected size (Fig. 1B). Moreover, the use of specific antibodies showed no cross-reactivity among the three proteins produced in the same system (Fig. 1C–E). Interestingly, the pharmacological characterization of Sv-IAG and Sv-TKIR revealed that the recombinant single-chain IAG ligand enhanced luciferase expression through its own cognate receptor (Fig. 4) and thus confirmed that the single-chain can bind the receptor and activate it, as has been previously reported for single-chain activation (Kristensen et al., 1995). We also found that human-insulin can activate Sv-TKIR (Fig. 4A). This result was not surprising since the recombinant human insulin is broadly employed and has undergone many alterations to improve potency, rendering it super potent (Kurtzhals et al., 2000).

Our receptor activation results confirm that the Sv-TKIR receptor signaling pathway is mediated through the MAPK/ERK pathway (Fig. 4A). This was further validated by the phosphorylation assays (Fig. 5) that confirmed that the rIAGs can activate this signaling pathway in a dose-dependent manner, as shown previously by Khalaila et al. (2002) who used crude AG extracts. The fact that both AG extract and rIAG evoke a similar response in the testicular tissue, further strengthens the notion that IAG is the sole key factor produced and secreted by the AG. Moreover, this activation demonstrates the presence of testicular receptors that can recognize an AG ligand, coinciding with the testis regression in response to IAG silencing (Rosen et al., 2010; Ventura et al., 2009).

The spatial expression profiles of *Sv-TKIR*, as indicated in Fig. 3, are in support of this testicular response. *Sv-TKIR* shows notable expression in the testis with basal expression in the neuroendocrine tissues of both sexes (BR and ES), muscle tissue (taken from the fifth walking leg, 5WL) ovary (OV) and the AG. This is evidence of how IAG can mediate testicular development *via* a paracrine pathway. Oddly, *Sv-TKIR* also expressed in the antennal glands (AnG), with the female AnG showing expression levels that exceed that of the male (Fig. 3A). In the context of this work, the explanation for this is yet to be elucidated. The expression of *Sv-TKIR* in the AnG is in support of our recent differential expression analyses of the *S. verreauxi* transcriptome, which clearly highlights the AnG as one of the principle tissues showing sex-related differential expression and a primary tissue for the expression of the identified sex-determining *Sv-Dmrts* (Chandler et al., 2016). Taken together, it appears clear that the AnG has a fundamental role in mediating the complex pathway of sexual development.

Expression of *Sv-TKIR* in female AnG, in the absence of the male-specific IAG, suggest that other, non-male specific ILP ligands (Chandler et al., 2015) act through this receptor in females. Nevertheless, although IAG has long been characterized as the male-specific masculinizing hormone (Ventura et al., 2011) there is growing evidence that IAG is also expressed in females. In female crayfish (Rosen et al., 2010), crab (Huang et al., 2014) and shrimp (Katayama et al., 2014) it has been demonstrated that IAG may have a function in the regulation of secondary vitellogenesis, through inhibition of the vitellogenin gene. In addition, it has also been suggested that IAG functions in glucose clearance and carbohydrate metabolism in the hepatopancreas of the female crab, *Callinetctes sapidus* (Chung, 2014), as well as a generic function in mediating molt-cycle in both sexes of the crab *Scylla paramamosain* (Huang et al., 2014).

This study enhances our understanding of the IAG endocrine axis. The discovery of Sv-TKIR, its expression profile and proof of its activation through the production of biologically-active rIAGs, is a significant milestone towards better understanding the mechanisms and pathways through which IAG mediates its masculinizing effects. Furthermore, the produced rIAGs can be used in the context of multiple "gain of function" experiments, combined with studies that explore temporal expression patterns of *Sv-TKIR* (and its decoy) with development, shedding more light on the

developmental timing and processes of masculinization as mediated by IAG.

Conflict of interest

The authors declare that they have no conflicts of interest with the contents of this article.

Author contributions

JA, JC, AE and TV designed and coordinated the study. JA and JC performed all experiments. JA and JC wrote the manuscript. AS provided the antibodies for Western blot analysis. All authors reviewed and edited the manuscript and approved the final version of the manuscript.

Acknowledgments

This research was supported by the Australian Research Council (http://www.arc.gov.au/) through a Discovery Early Career Research Award granted to Dr Tomer Ventura (DECRA; No. DE130101089), a Collaborative Research Network seed grant awarded to Dr Tomer Ventura and Professor Abigail Elizur and a University seed grant awarded to Dr Joseph Aizen, Dr Tomer Ventura and Professor Abigail Elizur (No. URG14/02). We gratefully acknowledge the Marie Curie International Research Staff Exchange Scheme Fellowship within the 7th European Community Framework Programme (612296-DeNuGReC).

Appendix A. Supplementary data

Supplementary data associated with this article can be found, in the online version, at http://dx.doi.org/10.1016/j.ygcen.2016.02.013.

References

Aizen, J., Kasuto, H., Golan, M., Zakay, H., Levavi-Sivan, B., 2007. Expression and characterization of biologically active recombinant tilapia FSH: immunohistochemistry, stimulation by GnRH and effect on steroid secretion. Biol. Reprod. 76, 692–700.

Aizen, J., Kowalsman, N., Kobayashi, M., Hollander, L., Sohn, Y.C., Yoshizaki, G., Niv, M.Y., Levavi-Sivan, B., 2012. Experimental and computational study of inter- and intra-species specificity of gonadotropins for various gonadotropin receptors. Mol. Cell. Endocrinol. 364, 89–100.

Aizen, J., Thomas, P., 2015. Role of Pgrmc1 in estrogen maintenance of meiotic arrest in zebrafish oocytes through Gper/Egfr. J. Endocrinol. 225, 59–68.

Boucher, P., Ditlecadet, D., Dube, C., Dufresne, F., 2010. Unusual duplication of the insulin-like receptor in the crustacean *Daphnia pulex*. BMC Evol. Biol. 10, 305.

Boucher, P., Ditlecadet, D., Dubé, C., Dufresne, F., 2010. Unusual duplication of the insulin-like receptor in the crustacean *Daphnia pulex*. BMC Evol. Biol. 10, 305–305.

Chandler, J.C., Aizen, J., Battaglene, S.C., Elizur, A., Ventura, T., 2016. Male sexual development and the androgenic gland: novel insights through the *de novo* assembled transcriptome of the Eastern spiny lobster, *Sagmariasus verreauxi*. Sexual Dev. http://dx.doi.org/10.1159/0000443943, in press.

Chandler, J.C., Aizen, J., Elizur, A., Hollander-Cohen, L., Battaglene, S.C., Ventura, T., 2015. Discovery of a novel insulin-like peptide and insulin binding proteins in the Eastern rock lobster *Sagmariasus verreauxi*. Gen. Comp. Endocrinol. 215, 76–87.

Charniaux-Cotton, H., 1954. Discovery in, an amphipod crustacean (*Orchestia gammarella*) of an endocrine gland responsible for the differentiation of primary and secondary male sex characteristics. C.R. Hebd. Seances Acad. Sci. 239, 780–782.

Chung, J.S., 2014. An insulin-like growth factor found in hepatopancreas implicates carbohydrate metabolism of the blue crab *Callinectes sapidus*. Gen. Comp. Endocrinol. 199, 56–64.

Cronin, L.E., 1947. Anatomy and histology of the male reproductive system of Callinectes sapidus Rathbun. J. Morphol. 81, 209–239.

Gurramkonda, C., Polez, S., Skoko, N., Adnan, A., Gabel, T., Chugh, D., Swaminathan, S., Khanna, N., Tisminetzky, S., Rinas, U., 2010. Application of simple fed-batch technique to high-level secretory production of insulin precursor using *Pichia pastoris* with subsequent purification and conversion to human insulin. Microb. Cell Fact. 9, 31.

Hasegawa, Y., Haino-Fukushima, K., Katakura, Y., 1987. Isolation and properties of androgenic gland hormone from the terrestrial isopod, *Armadillidium vulgare*. Gen. Comp. Endocrinol. 67, 101–110.

Huang, X., Ye, H., Huang, H., Yang, Y., Gong, J., 2014. An insulin-like androgenic gland hormone gene in the mud crab, *Scylla paramamosain*, extensively expressed and involved in the processes of growth and female reproduction. Gen. Comp. Endocrinol. 204, 229–238.

Hubbard, S.R., Till, J.H., 2000. Protein tyrosine kinase structure and function. Annu. Rev. Biochem. 69, 373–398.

Katayama, H., Hojo, H., Ohira, T., Ishii, A., Nozaki, T., Goto, K., Nakahara, Y., Takahashi, T., Hasegawa, Y., Nagasawa, H., Nakahara, Y., 2010. Correct disulfide pairing is required for the biological activity of crustacean androgenic gland hormone (AGH): synthetic studies of AGH. Biochemistry 49, 1798–1807.

Katayama, H., Kubota, N., Hojo, H., Okada, A., Kotaka, S., Tsutsui, N., Ohira, T., 2014. Direct evidence for the function of crustacean insulin-like androgenic gland factor (IAG): total chemical synthesis of IAG. Bioorg. Med. Chem. 22, 5783–5789.

Khalaila, I., Manor, R., Weil, S., Granot, Y., Keller, R., Sagi, A., 2002. The eyestalk–androgenic gland–testis endocrine axis in the crayfish *Cherax quadricarinatus*. Gen. Comp. Endocrinol. 127, 147–156.

Khayath, N., Vicogne, J., Ahier, A., BenYounes, A., Konrad, C., Trolet, J., Viscogliosi, E., Brehm, K., Dissous, C., 2007. Diversification of the insulin receptor family in the helminth parasite *Schistosoma mansoni*. FEBS J. 274, 659–676.

Kristensen, C., Andersen, A.S., Hach, M., Wiberg, F.C., Schäffer, L., Kjeldsen, T., 1995. A single-chain insulin-like growth factor I/insulin hybrid binds with high affinity to the insulin receptor. Biochem. J. 305, 981–986.

Kurtzhals, P., Schäffer, L., Sørensen, A., Kristensen, C., Jonassen, I., Schmid, C., Trüb, T., 2000. Correlations of receptor binding and metabolic and mitogenic potencies of insulin analogs designed for clinical use. Diabetes 49, 999–1005.

Lezer, Y., Aflalo, E.D., Manor, R., Sharabi, O., Abilevich, L.K., Sagi, A., 2015. On the safety of RNAi usage in aquaculture: the case of all-male prawn stocks generated through manipulation of the insulin-like androgenic gland hormone. Aquaculture 435, 157–166.

Li, F., Bai, H., Zhang, W., Fu, H., Jiang, F., Liang, G., Jin, S., Sun, S., Qiao, H., 2015. Cloning of genomic sequences of three crustacean hyperglycemic hormone superfamily genes and elucidation of their roles of regulating insulin-like androgenic gland hormone gene. Gene 561, 68–75.

Manor, R., Weil, S., Oren, S., Glazer, L., Aflalo, E.D., Ventura, T., Chalifa-Caspi, V., Lapidot, M., Sagi, A., 2007. Insulin and gender: an insulin-like gene expressed exclusively in the androgenic gland of the male crayfish. Gen. Comp. Endocrinol. 150, 326–336.

Martin, G., Juchault, P., Sorokine, O., Van Dorsselaer, A., 1990. Purification and characterization of androgenic hormone from the terrestrial isopod *Armadillidium vulgare* Latr. (Crustacea, Oniscidea). Gen. Comp. Endocrinol. 80, 349–354.

Martin, G., Sorokine, O., Moniatte, M., Bulet, P., Hetru, C., Van Dorsselaer, A., 1999. The structure of a glycosylated protein hormone responsible for sex determination in the isopod, *Armadillidium vulgare*. Eur. J. Biochem. 262, 727–736.

Maruyama, I.N., 2014. Mechanisms of activation of receptor tyrosine kinases: monomers or dimers. Cells 3, 304–330.

Okamoto, N., Nakamori, R., Murai, T., Yamauchi, Y., Masuda, A., Nishimura, T., 2013. A secreted decoy of InR antagonizes insulin/IGF signaling to restrict body growth in Drosophila. Genes Dev. 27, 87–97.

Okuno, A., Hasegawa, Y., Nishiyama, M., Ohira, T., Ko, R., Kurihara, M., Matsumoto, S., Nagasawa, H., 2002. Preparation of an active recombinant peptide of crustacean androgenic gland hormone1. Peptides 23, 567–572.

Okuno, A., Hasegawa, Y., Ohira, T., Katakura, Y., Nagasawa, H., 1999. Characterization and cDNA cloning of androgenic gland hormone of the terrestrial isopod *Armadillidium vulgare*. Biochem. Biophys. Res. Commun. 264, 419–423.

Rajpal, G., Liu, M., Zhang, Y., Arvan, P., 2009. Single-chain insulins as receptor agonists. Mol. Endocrinol. 23, 679–688.

Reddy Chichili, V.P., Kumar, V., Sivaraman, J., 2013. Linkers in the structural biology of protein–protein interactions. Protein Sci. 22, 153–167.

Rosen, O., Manor, R., Weil, S., Gafni, O., Linial, A., Aflalo, E.D., Ventura, T., Sagi, A., 2010. A sexual shift induced by silencing of a single insulin-like gene in crayfish: ovarian upregulation and testicular degeneration. PLoS ONE 5, e15281.

Shpilman, M., Hollander-Cohen, L., Ventura, T., Gertler, A., Levavi-Sivan, B., 2014. Production, gene structure and characterization of two orthologs of leptin and a leptin receptor in tilapia. Gen. Comp. Endocrinol. 207, 74–85.

Sroyraya, M., Chotwiwatthanakun, C., Stewart, M.J., Soonklang, N., Kornthong, N., Phoungpetchara, I., Hanna, P.J., Sobhon, P., 2010. Bilateral eyestalk ablation of the blue swimmer crab, *Portunus pelagicus*, produces hypertrophy of the androgenic gland and an increase of cells producing insulin-like androgenic gland hormone. Tissue Cell 42, 293–300.

Suzuki, S., Yamasaki, K., 1991. Sex-reversal of male *Armadillidium vulgare* (isopoda, malacostraca, crustacea) following andrectomy and partial gonadectomy. Gen. Comp. Endocrinol. 83, 375–378.

Veenstra, J.A., Rombauts, S., Grbić, M., 2012. In silico cloning of genes encoding neuropeptides, neurohormones and their putative G-protein coupled receptors in a spider mite. Insect Biochem. Mol. Biol. 42, 277–295.

Ventura, T., Aflalo, E.D., Weil, S., Kashkush, K., Sagi, A., 2011. Isolation and characterization of a female-specific DNA marker in the giant freshwater prawn *Macrobrachium rosenbergii*. Heredity 107, 456–461.

Ventura, T., Cummins, S.F., Fitzgibbon, Q., Battaglene, S., Elizur, A., 2014. Analysis of the central nervous system transcriptome of the Eastern rock lobster *Sagmariasus verreauxi* reveals its putative neuropeptidome. PLoS ONE 9, e97323.

Ventura, T., Fitzgibbon, Q., Battaglene, S., Sagi, A., Elizur, A., 2015. Identification and characterization of androgenic gland specific insulin-like peptide-encoding transcripts in two spiny lobster species: *Sagmariasus verreauxi* and *Jasus edwardsii*. Gen. Comp. Endocrinol. 214, 126–133.

Ventura, T., Fitzgibbon, Q.P., Battaglene, S.C., Elizur, A., 2015. Redefining metamorphosis in spiny lobsters: molecular analysis of the phyllosoma to puerulus transition in *Sagmariasus verreauxi*. Sci. Rep. 5, 13537.

Ventura, T., Manor, R., Aflalo, E.D., Weil, S., Khalaila, I., Rosen, O., Sagi, A., 2011. Expression of an androgenic gland-specific insulin-like peptide during the course of prawn sexual and morphotypic differentiation. ISRN Endocrinol. 2011, 476283.

Ventura, T., Manor, R., Aflalo, E.D., Weil, S., Raviv, S., Glazer, L., Sagi, A., 2009. Temporal silencing of an androgenic gland-specific insulin-like gene affecting phenotypical gender differences and spermatogenesis. Endocrinology 150, 1278–1286.

Ventura, T., Manor, R., Aflalo, E.D., Weil, S., Rosen, O., Sagi, A., 2012. Timing sexual differentiation: full functional sex reversal achieved through silencing of a single insulin-like gene in the prawn, *Macrobrachium rosenbergii*. Biol. Reprod. 86 (90), 91–96.

Ventura, T., Rosen, O., Sagi, A., 2011. From the discovery of the crustacean androgenic gland to the insulin-like hormone in six decades. Gen. Comp. Endocrinol. 173, 381–388.

Ventura, T., Sagi, A., 2012. The insulin-like androgenic gland hormone in crustaceans: from a single gene silencing to a wide array of sexual manipulation-based biotechnologies. Biotechnol. Adv. 30, 1543–1550.

Wang, Y., Liang, Z.-H., Zhang, Y.-S., Yao, S.-Y., Xu, Y.-G., Tang, Y.-H., Zhu, S.-Q., Cui, D.-F., Feng, Y.-M., 2001. Human insulin from a precursor overexpressed in the methylotrophic yeast *Pichia pastoris* and a simple procedure for purifying the expression product. Biotechnol. Bioeng. 73, 74–79.

Wen, Z., Gulia, M., Clark, K.D., Dhara, A., Crim, J.W., Strand, M.R., Brown, M.R., 2010. Two insulin-like peptide family members from the mosquito *Aedes aegypti* exhibit differential biological and receptor binding activities. Mol. Cell. Endocrinol. 328, 47–55.

Xie, T., Liu, Q., Xie, F., Liu, H., Zhang, Y., 2008. Secretory expression of insulin precursor in *Pichia pastoris* and simple procedure for producing recombinant human insulin. Prep. Biochem. Biotechnol. 38, 308–317.